Diffusively-driven overturning of a stable density gradient

by Andrew F. Thompson[1] and George Veronis[2]

ABSTRACT

We present the results of an experimental study on the formation and propagation of thermohaline intrusions from an initial state that is stably stratified in two diffusing components. The intrusions form in a layer that contains compensating horizontal gradients of the two components and that lies above a denser reservoir layer that is homogeneous. In the initial state, a vertical barrier separates the upper layer into two half layers each with a different concentration but with the same density. Differential diffusion of solute from the reservoir into the upper layer initiates intrusions that are separated by an interface and that move in opposite directions. The propagation of these intrusions is augmented by double-diffusive fluxes across the interface. Our experiments show that the formation of a diffusive interface between the two intrusions is a robust feature for all experiments that initially have a stable stratification in both diffusing components. A series of contrasting experiments with a fingering interface between the two intrusions was also performed using an initial density profile that favored fingering between part of the upper layer and the reservoir. A simple model is presented for intrusion propagation and density evolution in the intrusions, and the results are compared to measurements from the experiments. These experiments may help illuminate how thermohaline intrusions form in regions of the ocean where both temperature and salinity are stably stratified.

1. Introduction

Double diffusion (dd) is the term used to describe processes that involve the different rates of diffusion of two components in a fluid. It originated, more or less, in connection with oceanic phenomena (Stommel *et al.,* 1956) because the rate of diffusion of salt is about two orders of magnitude smaller than that of temperature. In most laboratory experiments either one of the components is unstably stratified while the remaining component and the overall density field are stable. Where the faster diffusing component is stable, so-called salt fingers (long, vertically slender structures) occur (Stern, 1960) and when the faster diffusing component is unstable, the instability takes the form of horizontal layers (Veronis, 1965). In both cases, diffusion of the faster diffuser plays an important role in releasing the potential energy of the unstable component. In the case of salt fingers when the fingers become long and strong enough, that structure becomes unstable and layers

1. Scripps Institution of Oceanography, University of California at San Diego, La Jolla, California, 92093-0213, U.S.A. *email: athompso@ucsd.edu*
2. Department of Geology and Geophysics, Yale University, New Haven, Connecticut, 06520-8109, U.S.A.

form, usually substantially thicker than the layers that form directly from the diffusive instability.

Although salt fingers have been observed in the ocean, the direct observation is a difficult one to make and it is much more common to deduce the presence of fingers indirectly from a vertical staircase structure that occurs, in which profiles show well-mixed layers of salt and temperature lying between thin regions of sharp gradients of salt and temperature. Staircases are observed in most parts of the ocean: in the upper, thermocline region in low latitudes, and over a greater range of depths in polar regions.

Both types of double-diffusive instability occur in the ocean but there is increasing evidence that a good deal of the staircase structure that is observed involves horizontal intrusions of water with the same density but with different concentrations of salt and temperature. The latter phenomenon is ubiquitous in the ocean. In fact, Merryfield (2000) has argued that lateral intrusions are essential for the formation of staircases. In a neat laboratory experiment, Ruddick and Turner (1979) demonstrated how intrusions occur when a barrier separating a stably stratified sugar (S) solution from a salt (T) solution of equivalent density was removed. The removal of the barrier disturbed the vertical interface between the two fluids and an interleaving of tongues of salt and tongues of sugar occurred. Subsequently, where a sugar tongue flowed over salt, fingers rained down into the salt layer, making the sugar layer lighter so that it flowed up the slope and the salt tongue heavier so that it flowed down the slope. Where a salt tongue penetrated over sugar, a thin diffusive interface formed. In terms of property distributions, a vertical profile shows a sequence of (sugar) finger layers sandwiched between diffusive interfaces.

The literature contains a large number of papers reporting double-diffusive processes in different parts of the ocean. In lower latitudes where surface waters are heated by the sun and evaporation takes place, the surface layers become warm and top-heavy in salt and salt fingers form. In polar latitudes warm, salty water intrudes under colder fresher water, thereby giving rise to diffusive instability. In addition to these one-dimensional (vertical) processes, there are intrusions involving both types of instability. Reported in the literature are cases where a mass of water with its own distribution of salt and heat somehow ends up next to another mass of water with different concentrations but with the same density. Interleaving then takes place.

Schmitt (1987) reports the best known example (C-SALT) of an area where salt fingers form and where horizontal intrusions also play a role. Carmack *et al.* (1997) describe examples of diffusive instability in arctic waters resulting from subsurface, horizontal intrusions of salty, warm water from the Atlantic.

Most of the oceanic observations of dd have been made in a region where one of the two components is unstably stratified. However, there have been citings of dd, evidenced by steps, in areas where both components appear to be gravitationally stably stratified. Foster and Carmack (1976) show one example from the Weddell Sea in their Figure 3. Joyce *et al.* (1978) show another, also from Antarctica. If the region where the two different stratifications merge is vertically thick, the instability that takes place could be consistent

with the one in the Ruddick-Turner experiment. However, Muench *et al.* (1990) report stable steps with a vertical scale of as little as one meter. Since the horizontal scale is of the order of kilometers, it seems unlikely that the structure originates from horizontal processes across a vertical surface.

In the present paper we report the results of an experiment that resembles the Ruddick-Turner experiment but with a denser base of water underneath: two homogeneous layers of equal density, one containing sugar (S) and the other salt (T), lying side by side, rest on a reservoir of much denser fluid consisting of higher concentrations of both salt and sugar. Thus, the stratification is stable in both components. After removal of the barrier (actually the layers are lowered past the barrier by draining some of the deep reservoir), an interleaving across the vertical interface can occur, but the process that is really responsible for the evolution is vertical diffusion across the horizontal interface: upward diffusion of salt creates a dense boundary layer at the bottom of the sugar half-layer which then slides in under the salt layer, thereby creating a field of motion, which evolves. We feel that this process may be pertinent for the situation observed in the stable regions sampled in the Antarctic.

In the next section we describe the experimental set-up and the procedures. The concentrations S and T in the upper layer are held constant from one experiment to the next but the concentrations in the underlying reservoir are varied so that the amount of diffusion of each concentration varies. In Section 3 we report our observations in those experiments. We observed the same qualitative behavior in all of these experiments; viz., the sugar layer always slid in under the salt layer, no matter how we varied the concentrations in the reservoir. Our efforts to obtain the opposite behavior (salty layer under sugar) are reported in Section 4. Some simple theory about the density of the intrusions and the intrusion lengths is given in Section 5 along with a few results. We finish with some concluding remarks in Section 6.

2. Experimental set-up

Before each experiment four solutions, corresponding to the four regions marked in Figure 1, were prepared using distilled water, pure cane sugar and kosher salt, which has no desiccant and gives a clearer solution. In all experiments solutions 1 and 2 were set to have a density of 1.02 g cm^{-3}, correct to $\pm 5 \times 10^{-6}$ g cm^{-3}, using an Anton Paar precision densitometer, with sugar in solution 1 and salt in solution 2. We refer to solutions 1 and 2 jointly as the upper layer. Solution 3 (the reservoir) was composed of both salt and sugar and had a density of 1.05 g cm^{-3} with the salt concentration having the same value as in solution 2, i.e. $T_3 = T_2$. Finally solution 4 (the bottom layer) had a density of 1.065 g cm^{-3} with T_4 contributing 1.02 g cm^{-3} as in solutions 2 and 3. The appropriate quantities of salt and sugar necessary to create these solutions were determined from the tables in Ruddick and Shirtcliffe (1979). The solutions were allowed to sit overnight to achieve room temperature. This minimized the effects of temperature fluctuations and heat diffusion in the experiments.
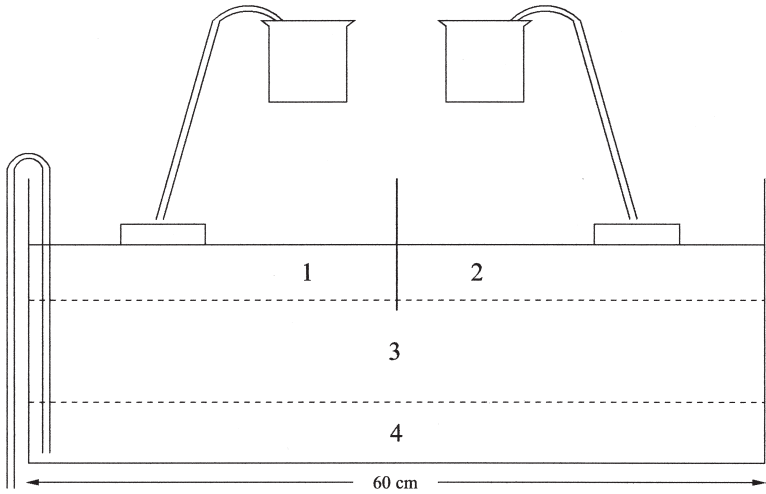
Figure 1. Diagram of laboratory equipment. Solutions 1 and 2 have the same density, but solution 1 contains only sugar and solution 2 contains only salt. Solution 3 is denser than 1 and 2, and solution 4 is denser still. In the main set of experiments both sugar and salt are stably stratified throughout the tank, and the salt concentrations are the same in solutions 2, 3 and 4. In later experiments the concentrations of solutions 3 and 4 are varied. Table 1 shows the density contributions of each diffusing component for the various experiments. A barrier separates solutions 1 and 2 before the start of the experiment. Fluid from region 4 is removed with a siphon to lower the surface and initiate the experiment.

The experiments were conducted in a Perspex tank 60 cm long, 20 cm deep and 10 cm wide. The tank was fitted with a lock gate that could be raised to any height and fixed in place with a small clamp. This gate was used to separate solutions 1 and 2 until the start of the experiment. Solutions 1 and 2 were added to the tank as depicted in Figure 1. The fluid was poured through siphons at a flow rate of approximately 3 mL s^{-1} onto sponges floating on the surface in order to minimize mixing. The thickness of the upper layer was varied slightly from one experiment to another; layers 3 and 4 were generally 1.5 to 2 cm thicker than the upper layer. Table 1 summarizes the approximate density contributions by each component in each layer for the different series of experiments.

In the main set of experiments the upper layer had a depth of approximately 2 cm. In these experiments the reservoir and lower layer contained the same amount of salt as solution 2 but they contained a larger concentration of sugar. This system allowed salt to diffuse preferentially into the sugary side of the upper layer.

The experiments were initiated using a new method for lock release. In previous lock-release experiments the barrier is pulled out of the tank manually or mechanically. Here we included layer 4 in order to be able to remove water from the experiment without disturbing the upper layers. We removed water from layer 4 by use of a siphon; this lowered the surface of the entire system at a slow rate until the surface was entirely below the barrier.

Table 1. Initial density contributions due to salt (T) and sugar (S) in the different solutions for the various experiments. The density is given by $\rho = \rho_0(1 + \alpha T + \beta S)$. The main experiments are described in detail in Section 3. Similar experiments show three examples of a series of experiments that were explored that exhibited the same features as the main experiments. The series of contrasting experiments are described in detail in Section 4.

	Solution 1	Solution 2	Solution 3	Solution 4
Main Expts.	$\beta S_1 = 0.02$ $\alpha T_1 = 0.0$	$\beta S_2 = 0.0$ $\alpha T_2 = 0.02$	$\beta S_3 = 0.03$ $\alpha T_3 = 0.02$	$\beta S_4 = 0.045$ $\alpha T_4 = 0.02$
Similar Expts.	$\beta S_1 = 0.02$ $\alpha T_1 = 0.0$	$\beta S_2 = 0.00$ $\alpha T_2 = 0.02$	$\beta S_3 = 0.05; 0.02; 0.05$ $\alpha T_3 = 0.02; 0.03; 0.0$	$\beta S_4 = 0.065; 0.02; 0.065$ $\alpha T_4 = 0.02; 0.045; \quad 0.0$
Contrast. Expts.	$\beta S_1 = 0.02$ $\alpha T_1 = 0.0$	$\beta S_2 = 0.0$ $\alpha T_2 = 0.02$	$\beta S_3 = 0.0$ $\alpha T_3 = 0.025 - 0.05$	$\beta S_4 = 0.0$ $\alpha T_4 = 0.4 - 0.065$

After initiation, measurements were made using a number of visualization techniques including shadowgraphs, still photography and time-lapse video. In all experiments, solution 1 was dyed blue, which allowed measurements to be made of the propagation of the intrusions as they formed. Flow visualization was also aided by dropping potassium permanganate crystals in the flow at different times during the experiment. Samples were removed at various locations and times using a syringe and density measurements were made using the precision densitometer.

3. Observations of main experiments

Once the fluid in the lowest layer and the reservoir was laid down in the tank, the sugary and salty solutions were added to the left and right sides of the barrier, respectively. Salt began to diffuse immediately from the reservoir into the sugary upper layer. Sugar also began to diffuse, but at a slower rate. Since T was the same in the salty upper layer and the reservoir ($T_2 = T_3$), no salt diffused upward to the right of the barrier. Therefore, the bottom of the sugary layer became denser than the salty layer. As fluid was siphoned out of the lowermost layer, the right and left sides of the upper layer came into contact (we denote that as time $t = 0$). Observations showed that the densities could be calibrated such that in most experiments there was a period of five to ten seconds where neither fluid showed a net propagation into the opposite region. This was then followed by a slight intrusion of the bottom of the sugary fluid (dyed blue) toward the right into the bottom of the salt layer. The shape of this intrusion was a very thin wedge with no turbulent motions apparent near the nose (Fig. 2a).

This intrusion of sugary fluid in turn induced a return flow of salty fluid into the left-hand side (the vertical plume to the left of the barrier in Fig. 2a). Because salty fluid pushed into a region with sugary fluid above it, sugar fingers formed causing vigorous convection just to the left of the barrier (Fig. 2b). The downward density flux due to the fingering caused lighter fluid to pool at the surface in the blue layer. Once reaching the surface, the lighter
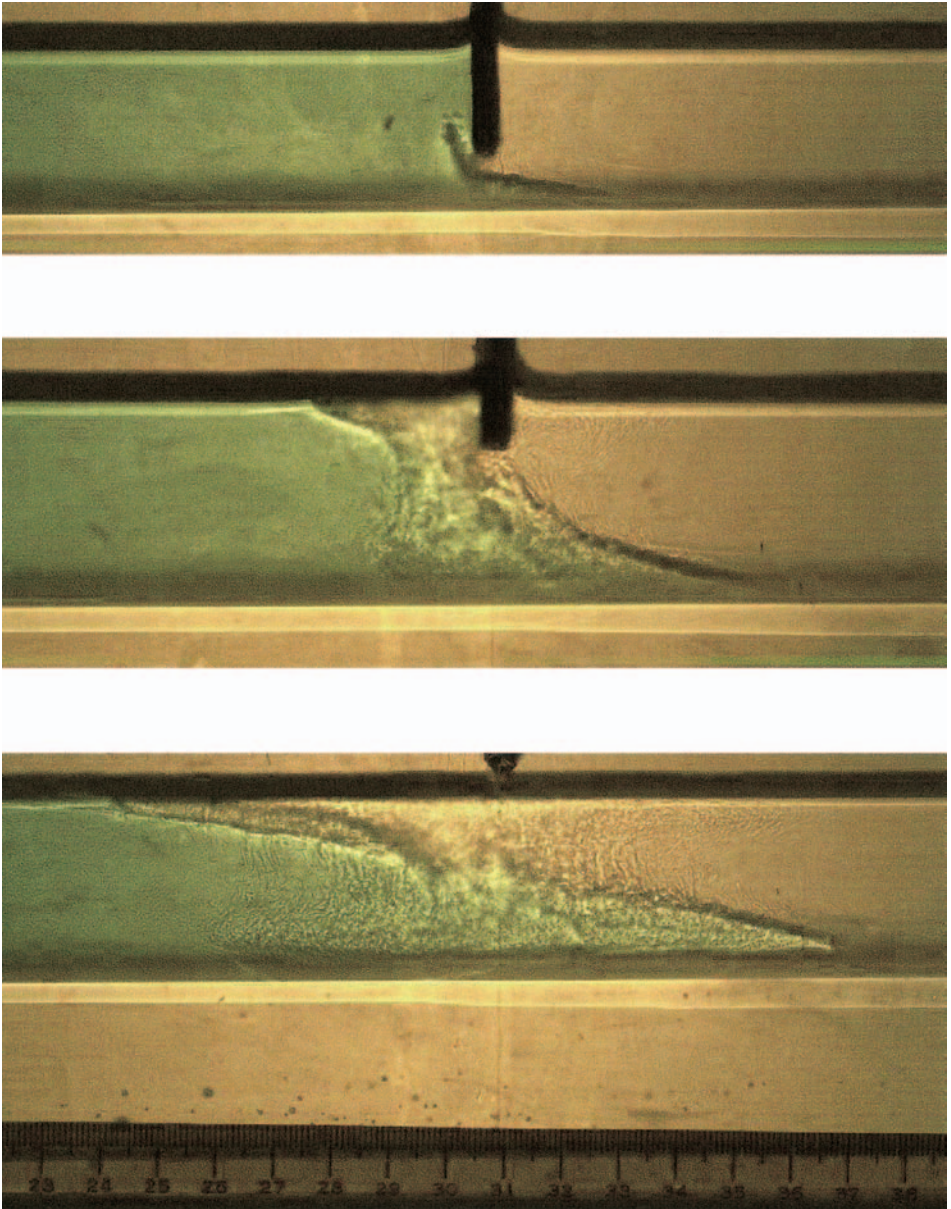
Figure 2. Photographs of initiation of a typical experiment at (a) $t = 58$ s, (b) $t = 122$ s, (c) $t = 184$ s.

fluid began to propagate to the left into the sugary region while remaining at the surface. While vigorous convection characterized the initiation of this experiment, the induced turbulence quickly resolved itself into a sharp diagonal diffusive interface that linked the
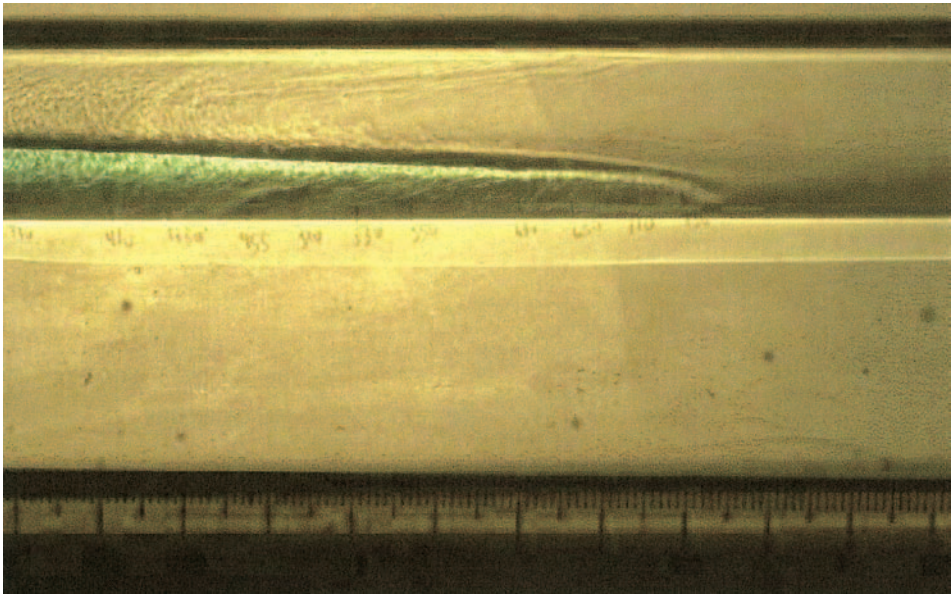
Figure 3. Photograph of the rightward-moving lower intrusion from the same experiment shown in Figure 2 at $t = 10:50$.

leftward moving upper intrusion and the rightward moving lower intrusion (Fig. 2c). Despite the vigorous convection, there still seemed to be minimal mixing of salty and sugary fluid as evidenced by the lack of mixing of the blue dye.

Once the sloping interface formed, strong convective plumes were observed both above and below the interface. These convective plumes are caused by the downward diffusion of salt across the sloping interface, thereby making fluid above the sloping interface lighter and the fluid below the interface denser. The accumulation of light fluid forced the tip of the salty wedge to move to the left and the denser fluid caused the tip of the blue wedge to move to the right.

As the lower, sugary intrusion received salt from both the lower reservoir and the fluid above, it continued to become denser and propagated to the right along the interface between the upper layer and the reservoir (Fig. 3). The current intruded as a wedge and did not exhibit the turbulent head common to gravity currents in a homogeneous ambient. The speed of the current was on the order of 1 cm min^{-1}, but moved more quickly when the depth of the upper layer was larger. The interface between the dyed lower intrusion and the clear upper intrusion appeared to be a straight line connecting the fronts, with some small curvature at the noses. We should note that the aspect ratio is quite small in these experiments. Furthermore, there is no initial vertical stratification in the upper layer so that we expect to see only a simple structure in the upper layer with one intrusion propagating to the right and one to the left.

The intrusion propagating to the left at the surface seemed to move at a nearly constant velocity that was also dependent on the height of the upper layer. In all experiments the leftward-moving intrusion hit the end wall first and generally did not seem to slow upon nearing the end wall. The rightward-moving lower intrusion did slow upon nearing the end wall. This was most likely due to a blocking flow caused by stratification established by diffusion from the reservoir into the upper layer to the right of the wedge.

In these experiments the interface between the salt and sugar layers remained sharp after the short initial period of mixing. Eventually, convection ran down and diffusion started to thicken the interface slowly. Convection was observed to occur in a region just above and just below the diagonal diffusive interface and took the form of tightly packed plumes. As convection began to run down, these devolved into isolated weak plumes with a separation of a few millimeters. These plumes were observed using a shadowgraph technique so it is not possible to describe any three-dimensional structure. The convective motions appeared to have a vertical length scale which was most likely determined by the shear in the two layers discussed below. Convection was not observed in a region extending a centimeter or two behind the head of the wedge (Fig. 3).

Besides the leftward- and rightward-propagation of the upper and lower intrusions respectively, there was also an overturning circulation within each layer. The sense of this circulation was clockwise in both layers and in general the velocities were greater than those of the intrusions. This feature was observed and commented upon by Ruddick *et al.* (1999). Visualization with the use of dye crystals revealed strong shear along the interface between the two regions of fluid as the horizontal velocity is to the left (up slope) in the clear, salt layer and to the right (down slope) in the blue-dyed, sugar layer. Return flows were to the right near the surface in the salt layer and to the left at the bottom of the sugar layer. Observations also indicated regions of high shear both near the surface and at the interface between the upper layer and reservoir. Dye crystals that fell through the upper layer showed that velocities in the reservoir were small compared to the velocities in the upper layer. While we expect no net transport over the entire height of the upper layer, as the system evolved there was a net transport of fluid to the left in the salt layer and a net transport to the right in the sugar layer since the sloping interface continued to flatten until it appeared horizontal.

Several different experiments, with different amounts of sugar in the reservoir, were carried out. All of them showed the same behavior; viz., penetration of sugary fluid from left to right between the salt layer and the reservoir. We also conducted a series of experiments in which the sugar density in the reservoir was maintained at 1.02 g cm^{-3} but the salt content was varied. In all of these experiments there was penetration of sugar water between the salt layer and the reservoir. We were unable to come up with a fully stable stratification in which salt penetrated under the sugar layer to produce sugar fingers. Therefore, if we are allowed to extrapolate these laminar results to the ocean, we conclude that the observation of layers in a fully stable system in the ocean is caused by diffusive

transport of heat across the thermal interface. This conclusion appears to be consistent with oceanic observations of layers formed in fully stable configurations.

4. Observations of contrasting experiments

In another series of experiments the reservoir and lower-layer solutions contained only salt. The reservoir density was varied systematically while the lowermost layer had a density 0.015 g cm^{-3} greater than the reservoir in each case. This created a gravitationally stable stratification that was favorable to fingering between the sugary upper layer and the reservoir. As expected, the strength and length scales of these fingers depended strongly on the density difference across the interface between the upper layer and the reservoir. In this section we consider the transition from weak fingering to strong fingering and discuss how this influenced intrusion formation in the upper layer.

In all these experiments fingering began as soon as the sugary fluid was laid down upon the reservoir. For experiments with $\delta\rho \geq 0.015$ g cm^{-3} between the upper layer and the reservoir, fingering was weak. The fingers grew slowly with time, but did not extend to the entire depth of the upper layer or the reservoir during the filling process (15–20 minutes). In this weak fingering regime, no flow was apparent in the reservoir. Upon removal of the barrier the weak-fingering experiments behaved like the main set of experiments described above. The blue sugary fluid intruded under the salty layer and propagated to the right. The interface between the two upper layer fluids sharpened and was characterized by a plume structure that appeared weaker than that of the previous experiments. The nose of the rightward-moving blue intrusion lifted slightly off the upper layer-reservoir interface, and some fingering could be observed below this intrusion. In the run-down stage of these experiments (approximately an hour or more), the left-hand side of the tank was characterized by fingers that extended from the surface almost to the bottom of the reservoir layer. These fingers were clearly sheared in both directions, exhibiting 2–3 complete sinusoids from the surface to the bottom of the reservoir.

Alternatively when $\delta\rho \leq 0.008$ g cm^{-3}, the fingering was vigorous during the filling process and the fingers extended from the surface to the base of the reservoir. The downward density flux caused by the fingering resulted in an overturning flow in the reservoir before the experiment was initiated. As the fingers fell on the left-hand side of the tank, the fluid became denser and moved as a gravity current along the interface between the reservoir and the lowermost layer. Due to the finite tank size, water near the top of the reservoir flowed back toward the left, where it ran under the sugary fluid and generated more fingers. This overturning circulation heightened the effect of the reservoir by continuously bringing fresh fluid into contact with the sugary layer leading to increased fingering, and also by bringing new salty water into contact with the salty region of the upper layer thus maintaining a high diffusion rate.

Due to the strong fingering, the sugary layer lost sufficient density so that after removal of the barrier it propagated to the right at the surface. This intrusion produced strong fingering along its bottom edge which dominated the dynamics in the upper layer. Salty

water also propagated to the left under the sugary fluid, but its progress could not be tracked because its structure was quickly overwhelmed by fingers. Strong shearing of the fingers was observable throughout the reservoir and the upper layer on the left side of the tank, though. The speed of the upper, sugary intrusion was faster than in experiments where the sugary intrusion was along the upper layer-reservoir interface. This was probably caused by both a lack of stratification near the surface and a larger density difference between the intrusion and its surroundings due to the fingering.

For experiments in between the weak- and strong-fingering regimes described here, the dynamics were not quite as clear. All the experiments in this intermediate range drove a flow in the reservoir due to the initial fingering, but the motion was typically weak and limited to a region extending approximately 5 to 10 cm on either side of the barrier. In the three experiments completed in this regime, three intrusions formed in the upper layer rather than two. After removal of the barrier, the blue sugary layer initially intruded below the salty layer causing a return flow of the salty layer. Unlike before, however, the salty fluid did not rise to the surface and a second thin sugary intrusion propagated to the right along the surface. Fingering was observed along the bottom of this upper intrusion, but the fingers were considerably weaker than those observed in the strong-fingering regime. The lower sugary intrusion propagated slowly in these experiments and stopped before reaching the end wall. In this transition regime it was difficult to separate the relative importance of effects caused by fingering during the filling process and by upper-layer interactions after removal of the barrier.

5. Basic theory

a. Initiation

We begin this section by writing down the governing equations for our experiment. We assume a two-dimensional, incompressible, Boussinesq salt and sugar system (T and S respectively). The equations of motion are given by

$$\psi_{zt} + J(\psi, \psi_z) = p_x/\rho_0 + \nu\nabla^2(\psi_z), \tag{1}$$

$$\psi_{xt} + J(\psi, \psi_x) = (-p_z - \rho g)/\rho_0 + \nu\nabla^2(\psi_x), \tag{2}$$

$$\xi_t + J(\psi, \xi) = -g(\alpha T_x + \beta S_x) + \nu\nabla^2\xi, \tag{3}$$

$$T_t + J(\psi, T) = \kappa_T\nabla^2 T, \tag{4}$$

$$S_t + J(\psi, S) = \kappa_S\nabla^2 S, \tag{5}$$

$$w = \psi_x, \quad u = -\psi_z, \quad \xi = \nabla^2\psi, \tag{6}$$

$$\rho = \rho_0(1 + \alpha T + \beta S), \tag{7}$$

where

$$\alpha = \frac{1}{\rho_0} \frac{\partial \rho}{\partial T}, \quad \beta = \frac{1}{\rho_0} \frac{\partial \rho}{\partial S} \tag{8}$$

are the coefficients of contraction of salt and sugar respectively and J represents the Jacobian, $J(A, B) = A_x B_z - A_z B_x$. These equations represent the conservation of momentum, horizontal vorticity, salt, sugar and mass, respectively. The full nonlinear and time-dependent equations are not easily solved either analytically or even numerically. Therefore, in the scope of this paper we have attempted to understand parts of the problem rather than a complete solution.

We first considered the initiation of the experiment by assuming that the barrier is removed instantaneously without any disturbances at time $t = 0$. Because of the differences in diffusion rates, we expect that at early times we can neglect the effects of sugar diffusion.

A relatively simple problem is to consider the horizontal diffusion of salt across the vertical interface separating the two regions in the upper layer. At early times we assume the nonlinear terms in the governing equations above are small and that across the front $\partial_x \gg \partial_z$. We simply solve the diffusion equation,

$$T_t = \kappa_T T_{xx} \tag{9}$$

with the boundary conditions $T \to 0$ as $x \to -\infty$ and $T \to T_0$ as $x \to +\infty$. Solving this equation gives us a solution in terms of the error function, but we will choose to solve the diffusion equation using Laplace transforms so we can use the solution in the momentum equation as well. After taking the Laplace transform of Eq. (9) and the boundary conditions, we find the solution in Laplace space is given by

$$\tilde{T} = \frac{T_0}{2s} \left(2 - \exp\left[-\sqrt{\frac{s}{\kappa_T}} x \right] \right) \quad x > 0 \tag{10}$$

$$\tilde{T} = \frac{T_0}{2s} \exp\left[\sqrt{\frac{s}{\kappa_T}} x \right] \quad x < 0. \tag{11}$$

Neglecting the nonlinear terms in the curl of the momentum equation and dropping derivatives with respect to z we seek to solve,

$$\psi_{xxt} = -g\alpha T_x + \nu\psi_{xxxx}. \tag{12}$$

Again we proceed by taking the Laplace transform of this equation, and apply the expression for $\tilde{T}$ we found above for $x > 0$. We can solve this equation for $\tilde{\psi}_{xx}$ and integrate once with respect to x. We then transform back to the time domain using the convolution theorem to find ψ_x or

$$w = \frac{g\alpha T_0}{2\nu} \left(\frac{1}{\kappa_T} - \frac{1}{\nu} \right)^{-1} \left(\int_0^t [\mathrm{erfc}(\eta_\nu) - \mathrm{erfc}(\eta_\kappa)] dt' \right), \quad x > 0, \tag{13}$$
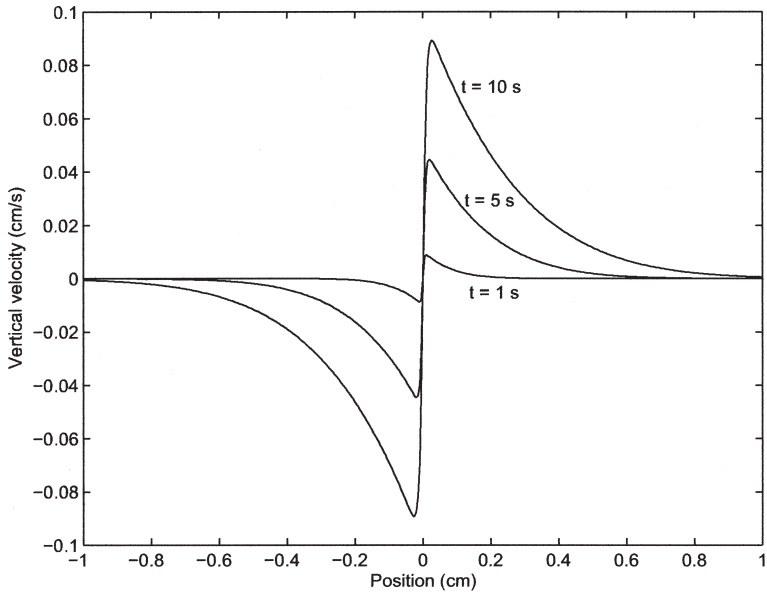
Figure 4. Plot of vertical velocity as a function of position from the vertical interface at various times after initiation caused by the horizontal diffusion of salt from positive x into negative x.

where $\eta_\nu = x/2\sqrt{\nu t'}$ and $\eta_\kappa = x/2\sqrt{\kappa_T t'}$. Using the same procedure we can determine the vertical velocity for $x < 0$, and find that it is just the opposite of (13). A plot of the vertical velocity as a function of distance from the interface at various times using parameters typical from our experiments is shown in Figure 4. As we expect, salt diffuses horizontally from positive to negative x increasing the density along $x < 0$, which drives a downward flow, but now reducing the density along $x > 0$, which drives an upward flow. This seems to indicate that an instability could occur even without the lower reservoir. We expect the reservoir to have a much larger effect because of the small aspect ratio and this was verified by our series of fingering experiments where the reservoir drove very different dynamics.

We next consider vertical diffusion of salt across the horizontal interface between the dense lower reservoir and the sugar solution in the upper layer. Once again we will neglect the effects of sugar diffusion and consider only vertical derivatives since they are much larger than the horizontal derivatives at early times. We consider the diffusion equation

$$T_t = \kappa_T T_{zz}, \tag{14}$$

which can be solved in terms of an error function. From this solution we can express the density in the upper layer as a function of vertical position and time. Using (7),

$$\rho = \rho_0(1 + \alpha T_0 + \alpha \delta T_0 \, \mathrm{erfc}(\eta_z)), \quad z > 0, \tag{15}$$

where $\eta_z = z/2\sqrt{\kappa_T t}$, and $z = 0$ is defined to be the interface between the upper layer and the reservoir. In (15), δT_0 represents the initial salinity difference between the reservoir and the upper sugar layer, $\delta T = T_3 - T_1$; later we will use ΔT to represent the difference in salinity between the salty and sugary upper layers. Finally, we have also used the fact that the initial concentrations in the two half layers are equal (i.e. $\beta S_0 = \alpha T_0$). The fact that (15) applies only for $z > 0$ reflects the assumption that concentrations in the reservoir are held fixed.

As a simple approximation at this point, we argue that the sugar region above the interface that gained salt through diffusion will intrude into the salt upper layer as a gravity current. The region of increased density is defined by the diffusive boundary layer which grows as $\sqrt{\kappa_T t}$. We can estimate the increase by taking the mean density increase across this boundary layer. We can then simplify the expression for the mean density change by assuming the profile is linear which gives

$$\delta\rho = \frac{\rho_0 \alpha \delta T_0}{2}. \tag{16}$$

A gravity current is characterized by the Froude number, $Fr = u/\sqrt{g'h}$, where $g' = g\delta\rho/\rho_0$ is the reduced gravity and we take the length scale h to be the diffusive length scale $\sqrt{\kappa_T t}$. Typically $Fr = 1$ at the nose of a gravity current propagating into a homogeneous ambient. In the process of filling the tank, though, some mixing occurs that leads to a thin region of stratification on both sides of the barrier. Ruddick *et al.* (1999) found that the velocity of intrusions propagating into a stratified ambient scaled like Nh, where N is the buoyancy frequency. That is the same as our definition of Fr. Ruddick *et al.* (1999) reported experimental velocities where

$$u \sim 0.005Nh, \tag{17}$$

which is much smaller than velocities predicted by the gravity current dynamics described above. The authors suggested that the smallness of the Froude number (0.005) was related to small deviations between the stratification within the intrusion and the background stratification. We provide an estimate of the Froude number in our experiments in Section 5c.

An important quantity in double-diffusive convection across a horizontal interface, or in our case the inclined interface between the two upper layers, is the flux ratio γ defined as

$$\gamma = -\frac{\beta F_S}{\alpha F_T} \tag{18}$$

for a diffusive interface, and the reciprocal of (18) for a fingering interface. Measurements of γ have shown that its value depends on the density ratio which is given by

$$R_\rho = \frac{\beta\Delta S}{\alpha\Delta T} \tag{19}$$

for a diffusive interface. For $R_\rho > 2$, Turner (1973) found that

$$\gamma = \sqrt{\frac{\kappa_S}{\kappa_T}}. \tag{20}$$

As R_ρ approaches 1, the value of γ also approaches 1. Turner interpreted the latter result by arguing that as R_ρ approaches 1, convection becomes more turbulent and therefore the same processes are transporting both diffusing components and the ratio of the fluxes are approximately equal. At the initiation of our experiments, the value of R_ρ has been carefully set to 1 so that density is compensated across the vertical front. As the interface flattens, the value of $\alpha \Delta T$ decreases (R_ρ increases) since salt diffuses downward into the sugar layer and the system becomes more stable. That behavior is consistent with behavior observed in a system with double diffusion across a horizontal interface.

b. Intrusion propagation

We note that the change in density in the salty upper layer is due to a flux of salt out and a smaller flux of sugar into this layer. We assume interaction between the salty upper layer and the reservoir is small. The change in density in the salty layer can be approximated by

$$\frac{d\rho_2}{dt} = -\alpha F_T \frac{1 - \gamma}{h_0/2}, \tag{21}$$

where ρ_2 is the density in the salty layer and h_0 is the initial depth of the upper layer. This model assumes that the layers are individually well mixed and that the density is a function of time only. The factor of 2 is a geometrical factor included because the layer depths are approximately equal at the midpoint. We note that this is a simplified model as our measurements have indicated that there are spatial gradients in the density field.

The flux of salt across the interface can be related to the change in salinity in the salty layer,

$$\alpha F_T = -\frac{\rho_0 h_0}{2} \frac{d}{dt} (\alpha T_2), \tag{22}$$

where T_2 is the salinity concentration in the salty layer. Finally, a third equation is needed as a parameterization of the salt flux as a function of the salt gradient (or difference across the interface). A review of flux laws for double diffusive convection across a diffusive interface is given in Kelley *et al.* (2003). For simplicity we use the flux relationship determined by Turner (1973) where he extended the flux law for turbulent convection

$$\alpha F_T = C(\alpha \Delta T)^{4/3}, \tag{23}$$

to apply to salt flux in double diffusion. Here $\Delta T = T_2 - T_1$, where T_1 is the salt concentration in the upper sugary layer, and C is a dimensional constant (like density $\times$

velocity) that depends on the solution properties and the density ratio R_ρ (Shirtcliffe, 1973).

We now need to write down the evolution equations for the sugary upper layer. The density increases in this layer due to both the downward double-diffusive flux of salt across the inclined interface and the upward diffusion of salt from the reservoir. This can be written as

$$\frac{d\rho_1}{dt} = \alpha F_T \frac{1 - \gamma}{h_0/2} + \frac{\alpha F_T^{diff.}}{h_0/2}, \tag{24}$$

where the diffusive flux is given by

$$\alpha F_T^{diff.} = \rho_0 \kappa_T \frac{\alpha(T_3 - T_1)}{h_m}. \tag{25}$$

This parameterization assumes that the salinity concentration of the reservoir T_3 is held fixed and that diffusion occurs across the thickness of the interface h_m, which is maintained at a constant value. We believe that this assumption may be valid while the shear at this interface is strong.

From the two flux relations we can write down the evolution equations for salinity in the two upper layers. They take the form

$$\frac{\rho_0 h_0}{2} \frac{d}{dt} (\alpha T_1) = C(\alpha \Delta T)^{4/3} + \frac{\rho_0 \kappa_T \alpha(T_3 - T_1)}{h_m}, \tag{26}$$

$$\frac{\rho_0 h_0}{2} \frac{d}{dt} (\alpha T_2) = -C(\alpha \Delta T)^{4/3}. \tag{27}$$

These equations were solved numerically using a second-order Runge Kutta scheme. The fluxes can also be computed at each time step using Eqs. (21) and (24), and the density in each layer can be determined. A fully diffusive system was also analyzed in which the flux parameterization across the inclined interface was modified from the four-thirds flux law given in (23) to the diffusive flux

$$\alpha F_T = \frac{\rho_0 \kappa_T \alpha \Delta T}{h_m}. \tag{28}$$

The numerical results and a discussion of the parameters used in the model can be found in Section 5c.

This spatially homogeneous model follows similar arguments made by Yoshida *et al.* (1987) for lock-exchange doubly diffusive gravity currents. In their model, there is no diffusive flux from the lower reservoir, and therefore the equations can be solved exactly. Neglecting the last term in (26), (26) and (27) can be integrated to give,

$$\alpha \Delta T = (\alpha \Delta T_0)(1 + t/\tau)^{-3}, \tag{29}$$

where τ is a time scale given by

$$\tau = \frac{3\rho_0 h_0}{4C(\alpha\Delta T_0)^{1/3}}. \tag{30}$$

Using (29) and the definition of the flux in (23), we can integrate to find the density in both the salty and the sugary upper layers. Following this method we find that the density difference across the inclined interface is given by

$$\Delta\rho = \rho_0(\alpha\Delta T_0)(1 - \gamma)(-1 + (1 + t/\tau)^{-3}), \tag{31}$$

where $\Delta\rho = \rho_2 - \rho_1$. Replacing the four-thirds flux parameterization with a purely diffusive parameterization, as in (28), we can follow the same steps as before to obtain

$$\alpha\Delta T = (\alpha\Delta T_0)\exp(-4\kappa_T t/h_0 h_m), \tag{32}$$

$$\Delta\rho = \rho_0(\alpha\Delta T_0)(1 - \gamma)(-1 + \exp[-4\kappa_T t/h_0 h_m]). \tag{33}$$

The results of these reservoir-absent systems are also discussed in Section 5c for comparison.

Both Maxworthy (1983) and Yoshida *et al.* (1987) have argued that the buoyancy force generated by density differences across the interface $(-\Delta\rho g(h_0/2)^2)$ is balanced by a double diffusive retarding force. This double diffusive force is given in Maxworthy (1983) as

$$F_{DD} = \rho UVL, \tag{34}$$

where L is the length of the intrusion and U and V are defined as

$$U = \frac{L}{t}, \quad V = \frac{\alpha F_T}{\rho\alpha\Delta T}. \tag{35}$$

If we apply the four-thirds flux law for αF_T, after setting the two forces equal, rearranging terms and making use of the definition of τ given in (30) we find

$$L \sim \left(\frac{\Delta\rho g h_0 \tau t}{3\rho_0}\right)^{1/2}\left(\frac{\alpha\Delta T}{\alpha\Delta T_0}\right)^{-1/6}. \tag{36}$$

Alternatively, applying the diffusive flux law (28), we find that

$$L \sim \left(\frac{\Delta\rho g h_0^2 h_m t}{4\rho_0\kappa_T}\right)^{1/2}. \tag{37}$$

The reservoir-absent solutions for $\Delta\rho$ and $\alpha\Delta T$ with the four-thirds flux parameterization, (31) and (29) respectively, can then be substituted into (36), which gives an analytic solution for the growth of L:

$$L \sim [(\alpha\Delta T_0)(1 - \gamma)g h_o \tau]^{1/2} \times [t(1 + t/\tau)(1 - (1 + t/\tau)^{-3})]^{1/2}. \tag{38}$$
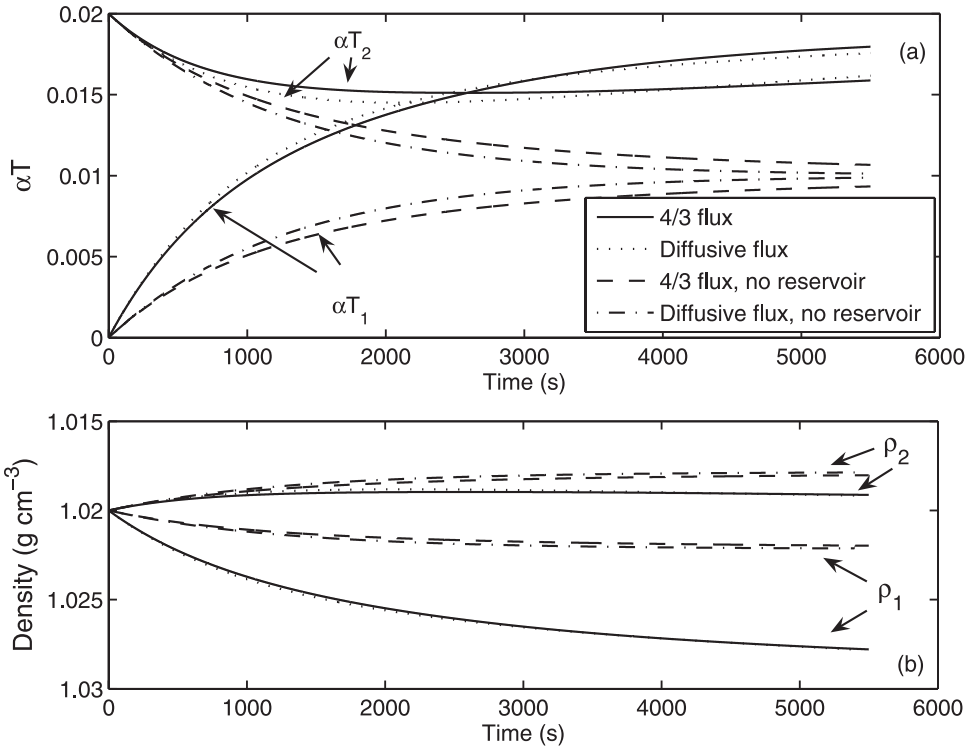
Figure 5. Numerical simulations of (a) αT and (b) density ρ in the sugary (1) and salty (2) upper layers. The parameters are the same as for the main experiments (Table 1) with $h_0 = 2$ cm. Results are shown for both a four-thirds and a diffusive flux parameterization across the inclined interface, with and without the effects of the reservoir. Density increases downward along the y-axis.

Yoshida et $al.$ (1987) have shown that in this case the intrusion grows linearly with time for both $t \ll \tau$ and $t \gg \tau$. Using the temperature and density evolution equations for the diffusive flux parameterization (32) and (33), the scaling for L becomes

$$L \sim [(\alpha \Delta T_0)(1 - \gamma)gh_0^2 h_m/\kappa_T]^{1/2} \times [t - t \exp(-4\kappa_T t/h_0 h_m)]^{1/2}, \qquad (39)$$

where in this case, $L \sim t$ at early times and $L \sim t^{1/2}$ at long times.

c. Results

As mentioned above, the dynamics of these experiments were robust in all runs where both components were originally stably stratified. We present a few brief results here based on variations of the initial condition such as upper layer depth and salt/sugar concentrations in the upper layer. We emphasize, though, that the main features described in Section 3 occurred in all experiments.

In Figure 5 we show the results of the numerical simulations of the evolution equations

for salinity and density in the two upper layers. The initial parameters are the same as in the main experiments (Table 1) with $h_0 = 2$ cm. Figure 5a shows salinity concentrations in the sugary (1) and salty (2) upper layers for both the four-thirds and diffusive flux parameterizations. The analytical solutions in the absence of the reservoir are also shown for comparison. The figure shows that the addition of the reservoir has a significant effect on the mean salinity value in the two layers. The simulations also show that when the reservoir is present, the salinity in the sugary layer eventually exceeds that of the salty layer. At this point the flux across the inclined interface is no longer doubly diffusive. The flux laws were not modified in this simple model (which is already over-simplified by only tracking salinity explicitly and ignoring spatial gradients). After this point the salinity increased in both layers due to the flux of salt in from the reservoir.

In Figure 5b we show the evolution of the densities in the upper layers (density increases downward). The effect of the reservoir leads to a much larger change in the density of the sugary layer. The slow increase in density in the salty layer over the later part of the simulations is due the change in sign of ΔT (Fig. 5a), and is most likely not a physical result. Note that density increases downward along the y-axis.

This model provides only a rough estimate of the physical processes occurring in our experiments as evidenced by the strong vertical structure of the density seen in Figure 6, which shows density measurements taken at various heights and times from a single experiment with the same parameters as the simulations. All measurements were taken from the horizontal center of the tank and their heights are described in the key of Figure 6. As expected, density decreased steadily in the upper salty layer and increased steadily in the lower sugary layer. Measurements made just above and below the interface (regions B and C) seem to reach a quasi-equilibrium state after approximately 1500–2000 seconds, while measurements taken near the surface and near the reservoir interface reach nearly steady values after about 4000 seconds. These measurements show that despite the convection observed in the experiments, there may be either a staircase or a stratified density profile. The vertical density structure could depend strongly on the overturning circulation that is observed. The density change at region D is the largest because of the continuous diffusion of salt into this region from the lower reservoir. The solid and dashed lines show the density evolution in the two upper layers (Fig. 5b) using the four-thirds-flux and the diffusive-flux parameterization for comparison.

If we neglect the reservoir and consider Eqs. (31) and (33) we can see that the run-down time for the density jump across the interface is roughly τ for the four-thirds flux law or $h_0 h_m / 4\kappa_T$ for the diffusive flux law. The value of τ can be determined from (30), although determining C is somewhat difficult because there are large fluctuations in its value for $1 < R_\rho < 2$ (Turner, 1973). Huppert (1971) suggests that C is roughly four times the value of the coefficient of the four-thirds flux law in the case with solid boundaries when $R_\rho = 1$. Applying this argument we find that C is roughly 0.04 g cm^{-2} s^{-1} (see Turner, 1973, Eq. 7.1.10) and using parameters from our experiments $\tau \sim 150$ s. However, because of the great uncertainty about the correct value of C near $R_\rho = 1$, we have experimented with
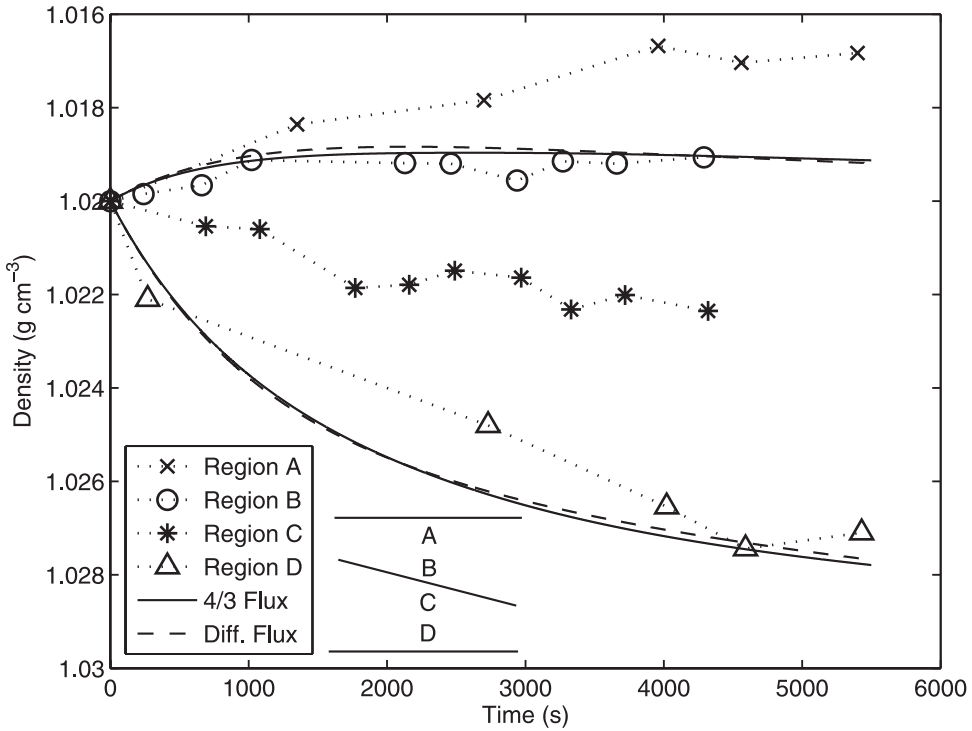
Figure 6. Density measurements as a function of time from a single experiment. The symbols refer to different heights where samples were removed as indicated in the key above. All samples were removed from the center of the tank. Density increases downward along the y-axis. The solid and dashed lines show the density evolution of the two layers based on the numerical simulation with a four-thirds flux and a diffusive flux parameterization, respectively.

different values to find a close fit to the data. We found that $C = 8 \times 10^{-4}$ g cm^{-2} s^{-1} gives a good fit and we show the corresponding curve in Figure 6 along with the diffusive curve. The run-down time for the diffusive parameterization is given by

$$\frac{h_0 h_m}{4\kappa_T} \sim \frac{1 \text{ cm}(.05 \text{ cm})}{4(1 \times 10^{-5} \text{ cm}^2 \text{ s}^{-1})} \sim 1.3 \times 10^3 \text{ s}.$$

If, on the other hand, the initial estimate of τ (150 s) is accurate, then a four-thirds type turbulent flux may quickly bring the salt and sugar concentrations to near equilibrium with little changes in the density, and later changes in the densities of the upper layers may be related to a diffusive type flux. This is further supported by the fact that at the initiation of our experiment, $R_\rho = 1$ at which point γ also approaches 1. Measurements of the separate salt and sugar concentrations fields would be necessary to examine this issue fully.

Because of the vertical variation in ρ it does not make sense to define a run-down $\Delta\rho$ across the interface. We do note, though, that in another set of experiments where the initial
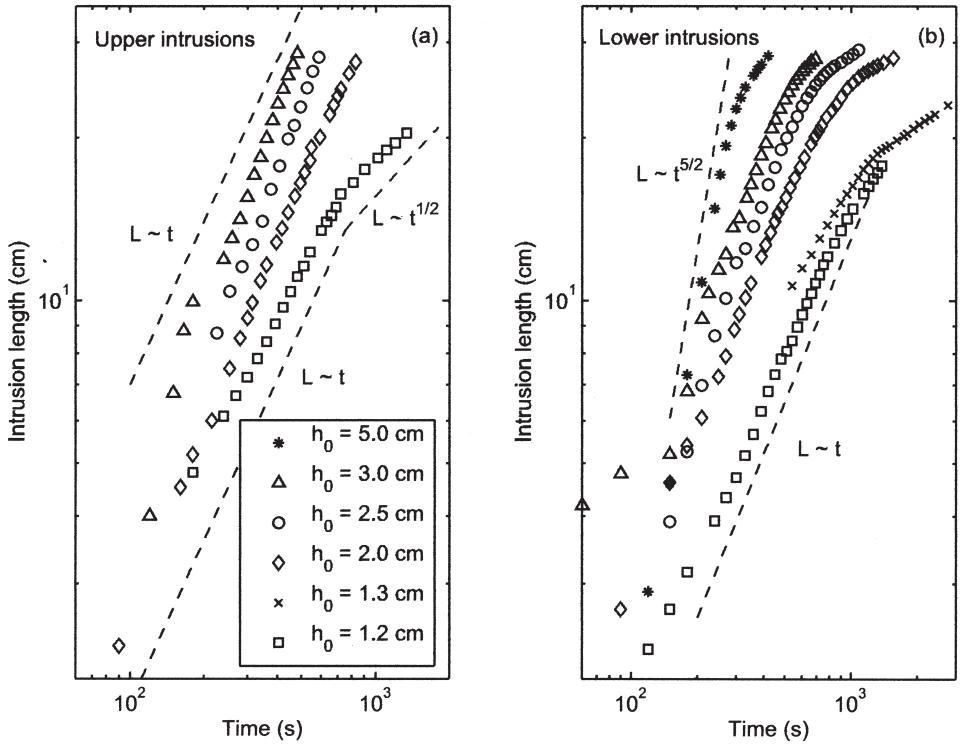
Figure 7. Position of the (a) upper and (b) lower intrusion fronts in the main experiments as a function of time for various upper layer depths. Power law relations are shown with dashed lines for reference.

concentration difference in the upper layer was reduced by a third ($\alpha \Delta T_0 = 0.0067$), the relative variation in density between the different layers at run-down was roughly a third of the density differences for the case where $\alpha \Delta T_0 = 0.02$. This agrees well with the reservoir-absent theory that the run-down density jump across the interface should scale linearly with $\alpha \Delta T_0$.

Figures 7a and 7b show measurements of the front positions, determined from visual observations, of the upper and lower intrusions respectively as a function of time. All experiments had an upper layer density of 1.02 g cm^{-3} and a reservoir density of 1.05 g cm^{-3}. The various symbols represent different initial depths of the upper layer h_0. From both figures it is clear that the intrusion velocity increases as the layer depth increases. Both figures have log-log axes and various power law relations are shown with dashed lines for reference. The length of the upper intrusion seems to depend linearly on time, so that the velocity is constant. There are no pronounced end wall effects, although there may be some late-time behavior and a change in regime for the slowest experiment where $h_0 = 1.2$ cm. Most of the measurements of the lower intrusions indicate that the

velocity is approximately constant, although there does seem to be a monotonic increase in slope in Figure 7b with increasing layer depth. There is a much more pronounced end wall effect in the lower-layer intrusion due to stratification generated at the upper layer–reservoir interface when filling the tank. This leads to a blocking flow, which feels the presence of the end wall much earlier than the upper intrusion (Browand and Winant, 1972).

Velocities were roughly on the order of 0.02 cm s^{-1}. If we estimate a value of N based on pure salt diffusion over the diffusive boundary layer (Section 5a), then using $t = 600$ seconds, we find $Fr \sim 0.02$, which falls between the gravity current ($Fr = 1$) and Ruddick *et al.* (1999) ($Fr = 0.005$) limits. This is a difficult estimate, though, due to the diffusive mixing that occurs during the filling process. Finer scale density measurements in both layers would be needed to arrive at a more accurate estimate of the Froude number.

6. Discussion

In this study we have attempted to show how horizontal thermohaline intrusions may develop in the absence of a stratification that allows for double-diffusive convection. The problem was studied experimentally using sugar and salt solutions. We found that when the faster diffusing component diffuses preferentially into the part of the upper layer containing the slower diffuser, it generates a horizontal motion into the part of the upper layer containing the faster diffuser. Horizontal intrusions form and then become strengthened by dd. The method we chose to show this process was to allow properties to diffuse out of a reservoir underlying the intrusion region. We also varied the reservoir properties and were able to show that the behavior that we report was very robust with respect to the reservoir properties.

Our experiments also showed that an underlying reservoir changes the dynamics considerably. The motion is not generated by random perturbations but rather by the vertical diffusion just described and a diffusive interface is formed between the two components. This behavior is different from the original experiments of Ruddick and Turner (1979) where fingering interfaces dominated the dynamics. We also note that many intrusions were formed in the Ruddick and Turner (1979) experiments because their fluid was deep and initially stratified. In those of our experiments where fingering occurred prior to removing the barrier, more than two intrusions were observed when the upper layer is deep (results not reported).

A number of important questions remain, especially concerning the overturning circulations within the intrusions and how salt and sugar are exchanged across the intrusion interface. Unfortunately in the scope of these experiments we were unable to measure salt and sugar concentrations separately. This information would improve our understanding of the fluxes between the two layers as they move past one another creating strong shear.

Of course, we have not tried to create a simulation of dd in the ocean. Our use of salt and sugar with diffusivity ratio (3:1) rather than heat and salt (100:1) is convenient in the laboratory and avoids the problem associated with heat losses to the environment. Our use

of shallow layers helps to isolate the role of vertical diffusion as a determining process in the generation of horizontal intrusions, particularly in regions where shallow layers of fluid occur with both components stably stratified, as has been observed in the Southern Ocean away from lateral boundaries. The role of vertical diffusion is important in any gravitationally stable set up with warm salty water underlying cold fresh water but its role in generating horizontal intrusions has generally not been appreciated.

It is very significant that no matter how we arranged the initial distributions in the stable stratifications in the reservoir and in the overlying layers, as the initially vertical interface between the sugar and the salt layers turned toward the horizontal, a diffusive interface formed. We were never successful in our efforts to establish a finger interface until we incorporated an unstable stratification in the initial sugar distribution. Thus, this preference for a diffusive interface is a robust feature of the fully stably stratified system. A strong shear necessarily occurs across the interface in the upper layer and it is known (Linden, 1974) that finger transports are inhibited by shear. Although that may be an additional reason for the suppression of a finger interface, it is clear from the physical behavior of the system that vertical diffusion favors the formation of a diffusive interface.

In discussing the effects of vertical diffusion on dd systems we have confined our study to fully stable configurations. In addition to the few observations of fully stable layers in polar latitudes, outflows of river waters are candidates. However, the effect is also important in any two-component system in which density is stable, although the behavior that we described may be modified by dd convection. Intrusions of salty warm water that find their density level, such as those by Mediterranean water into the Atlantic or by North Atlantic water into the Arctic, will generate denser water at the top and bottom of the intrusions themselves. Lateral interaction with adjacent, ambient water will be modified by the Coriolis force but any response must involve horizontal density contrasts that result from vertical diffusion.

REFERENCES

Browand, F. K. and C. D. Winant. 1972. Blocking ahead of a cylinder moving in a stratified environment: An experiment. Geophys. Fluid Dyn., *4,* 29–53.

Carmack, E. C., K. Aagaard, J. H. Swift, R. W. MacDonald, F. A. McLaughlin, E. P. Jones, R. G. Perkin, J. N. Smith, K. M. Ellis and L. R. Killius. 1997. Changes in temperature and tracer distributions within the Arctic Ocean: Results from the 1994 Arctic Ocean section. Deep-Sea Res. II, *44,* 1487–1502.

Foster, T. D. and E. C. Carmack. 1976. Temperature and salinity structure in the Weddell Sea. J. Phys. Oceanogr., *6,* 36–44.

Huppert, H. E. 1971. On the stability of a series of double-diffusive layers. Deep-Sea Res., *18,* 1005–1021.

Joyce, T. M., W. Zenk and J. M. Toole. 1978. The anatomy of the Antarctic Polar Front in the Drake Passage. J. Geophys. Res., *83,* 6093–6113.

Kelley, D. E., H. J. S. Fernando, A. E. Gargett, J. Tanny and E. Ozsoy. 2003. The diffusive regime of double-diffusive convection. Prog. Oceanogr., *56,* 461–481.

Linden, P. F. 1974. Salt fingers in a steady shear flow. Geophys. Fluid Dyn., *6,* 1–27.

Maxworthy, T. 1983. The dynamics of double-diffusive gravity currents. J. Fluid Mech., *128,* 259–282.

Merryfield, W. J. 2000. Origin of thermohaline staircases. J. Phys. Oceanogr., *30,* 1046–1068.

Muench, R. D., H. J. S. Fernando and G. R. Stegen. 1990. Temperature and salinity staircases in the Northwestern Weddell Sea. J. Phys. Oceanogr., *20,* 295–306.

Ruddick, B. R., O. M. Phillips and J. S. Turner. 1999. A laboratory model of finite-amplitude thermohaline intrusions. Dyn. Atmos. Oceans, *30,* 71–99.

Ruddick, B. R. and T. G. L. Shirtcliffe. 1979. Data for double diffusers: Physical properties of aqueous salt-sugar solutions. Deep-Sea Res., *26A,* 775–787.

Ruddick, B. R. and J. S. Turner. 1979. The vertical length scale of double-diffusive intrusions. Deep-Sea Res., *26A,* 903–913.

Schmitt, R. W. 1987. The Caribbean Sheets and Layers Transects (C-SALT) Program. EOS, Trans., Amer. Geophys. Union, *68,* 57–60.

Shirtcliffe, T. G. L. 1973. Transport and profile measurements of the diffusive interface in double diffusive convection with similar diffusivities. J. Fluid Mech., *57,* 27–43.

Stern, M. E. 1960. The "salt fountain" and thermohaline convection. Tellus, *12,* 172–175.

Stommel, H., A. B. Arons and D. Blanchard. 1956. An oceanographical curiosity: the perpetual salt fountain. Deep-Sea Res., *3,* 152–153.

Turner, J. S. 1973. Buoyancy Effects in Fluid, Cambridge University Press, 368 pp.

Veronis, G. 1965. On finite amplitude instability in thermohaline convection. J. Mar. Res., *23,* 1–17.

Walsh, D. and E. Carmack. 2002. A note on the evanescent behavior of Arctic thermohaline intrusions. J. Mar. Res., *60,* 281–310.

Yoshida, J., H. Nagashima and W. Ma. 1987. A double diffusive lock-exchange flow with small density difference. Fluid Dyn. Res., *2,* 205–215.